

This document contains a post-print version of the paper

Constrained model predictive manifold stabilization based on transverse normal forms

authored by **Martin Böck and Andreas Kugi**
and published in *Automatica*.

The content of this post-print version is identical to the published paper but without the publisher's final layout or copy editing. Please, scroll down for the article.

Cite this article as:

M. Böck and A. Kugi, "Constrained model predictive manifold stabilization based on transverse normal forms", *Automatica*, vol. 74, pp. 315–326, 2016. DOI: [10.1016/j.automatica.2016.07.046](https://doi.org/10.1016/j.automatica.2016.07.046)

BibTex entry:

```
@Article{acinpaper,  
  Title = {Constrained model predictive manifold stabilization based on transverse normal forms},  
  Author = {Martin B{\o}ck and Andreas Kugi},  
  Journal = {Automatica},  
  Year = {2016},  
  Pages = {315--326},  
  Volume = {74},  
  Doi = {10.1016/j.automatica.2016.07.046}  
}
```

Link to original paper:

<http://dx.doi.org/10.1016/j.automatica.2016.07.046>

Read more ACIN papers or get this document:

<http://www.acin.tuwien.ac.at/literature>

Contact:

Automation and Control Institute (ACIN)
TU Wien
Gusshausstrasse 27-29/E376
1040 Vienna, Austria

Internet: www.acin.tuwien.ac.at
E-mail: office@acin.tuwien.ac.at
Phone: +43 1 58801 37601
Fax: +43 1 58801 37699

Copyright notice:

This is the authors' version of a work that was accepted for publication in *Automatica*. Changes resulting from the publishing process, such as peer review, editing, corrections, structural formatting, and other quality control mechanisms may not be reflected in this document. Changes may have been made to this work since it was submitted for publication. A definitive version was subsequently published in M. Böck and A. Kugi, "Constrained model predictive manifold stabilization based on transverse normal forms", *Automatica*, vol. 74, pp. 315–326, 2016. DOI: [10.1016/j.automatica.2016.07.046](https://doi.org/10.1016/j.automatica.2016.07.046)

Constrained Model Predictive Manifold Stabilization Based on Transverse Normal Forms [★]

Martin Böck ^a, Andreas Kugi ^a

^a*Automation and Control Institute, TU Wien, Gußhausstr. 27–29, 1040 Vienna, Austria*

Abstract

The optimization-based stabilization of manifolds for nonlinear dynamical systems with constraints is investigated. Manifolds in the state or output space are considered for which the original system description can be transformed into a so-called transverse normal form. With this formulation, the motion of the system transverse and tangential to the manifold can be separately described. The transverse normal form is combined with a tailored model predictive control scheme to achieve the objectives of stabilizing the manifold, rendering it invariant, and imposing a desired motion on the manifold under due consideration of constraints. Furthermore, the stabilization of the manifold is prioritized over the movement on the manifold. Convergence of the model predictive control scheme is proven. The applicability of the proposed concept is demonstrated by an illustrative simulation example.

Key words: Input constraints; Manifold stabilization; Model predictive control; Transverse normal form.

1 Introduction

The stabilization of manifolds or sets is a popular field in modern control theory. It can be seen as an extension of the classical task of set point stabilization as a set point constitutes a manifold of dimension zero. Typically, manifolds defined in the output or state space of a dynamical system are considered, see, e.g., [28]. Roughly speaking, the goal of manifold stabilization is to ensure (asymptotic) convergence of the output or state of the system to the manifold. Moreover, the resulting controller is frequently supposed to achieve two further objectives. Firstly, the (tangential) movement on the manifold should be of a desired form, and the second objective is the so-called invariance property. Roughly speaking, it states that if at any given point in time the system is exactly on the manifold, or more precisely in a corresponding controlled invariant subset of the state space, then the manifold must never be left again in the nominal, undisturbed case. The invariance property is required to hold regardless of the tangential movement, cf. [29]. In the following, unless stated otherwise, the term manifold stabilization not only refers to the stabilization

itself but also includes the task of achieving a desired movement on the manifold.

One possibility is to tackle these tasks from a geometric point of view. For example, in [28] and [30] the stabilization of controlled invariant submanifolds of the state space of control-affine dynamical systems is investigated. To this end, the system description is transformed into a so-called transverse normal form (TNF). The TNF consists of two sets of coordinates describing the transverse and tangential motion with respect to the manifold. By rendering the transverse dynamics asymptotically stable the manifold is stabilized. The invariance property is fulfilled and the motion on the manifold can be influenced by controlling the tangential dynamics. However, the consideration of system constraints is not possible in a straightforward way.

There are many works dealing with the stabilization of invariant sets for passive systems. Typically, the sets to be stabilized are subsets of the zero level set of the storage function, see, e.g., [11] and [33]. In [12] passive systems in control-affine form are considered and the stabilization of open-loop positively invariant subsets of the zero level set of the storage function is investigated. The authors in [34] deal with the stabilization of the zero level set of a nonnegative objective function under nonlinear system dynamics. It is shown that there exist controllers providing arbitrarily small input values for sta-

[★] This paper was not presented at any IFAC meeting. Corresponding author M. Böck. Tel. +43 1 58801 376268. Fax +43 1 58801 9376268.

Email addresses: boeck@acin.tuwien.ac.at (Martin Böck), kugi@acin.tuwien.ac.at (Andreas Kugi).

bilizing the set, i.e., input constraints can in principle be respected by a suitable control law. In these works, the movement of the system in the set is not taken care of.

The stabilization of sets in the context of haptic simulators is investigated in [37]. Similar to the works of Nielsen et al. the main ideas are based on projection techniques and TNFs. In [4] a method is presented for stabilizing manifolds in flat output spaces. The movement on the manifolds can be chosen freely and the invariance property is fulfilled. However, system constraints cannot be systematically respected.

The authors in [22] show that uniform global asymptotic controllability to a closed set implies the existence of a locally Lipschitz control Lyapunov function (CLF). Based on this CLF a robust feedback law for stabilizing the set is constructed. In [2] time-varying systems are considered. Similar to [22] it is shown that the existence of a continuous CLF with respect to a closed subset of the state space is equivalent to the global asymptotic controllability to that set. The authors in [26] provide sufficient stability criteria for time-varying sets in the state space of nonlinear time-varying systems using vector Lyapunov functions. Based on these results a stabilizing feedback is developed for multi-agent dynamical systems and applied to multi-vehicle formation control. The asymptotic stabilization of subsets of the state space of systems with positive inputs is investigated in [19]. The proposed control law can also be applied to positive systems as a special case.

In [16] sampled-data open-loop feedbacks are considered. For using this type of feedback, convergence conditions of the state of a nonlinear system to a compact set are derived. Constraints on inputs and states are taken into account. The class of sampled-data open-loop feedbacks includes model predictive control (MPC). MPC relies on solving an optimal control problem (OCP) at each sampling instant to determine the control input for the system, see, e.g., [3], [31]. The convergence conditions obtained in [16] are applied to MPC as well. In contrast to this work, the movement of the system in the set is not taken care of and the target set is defined as compact subset of the state space. In this paper, manifolds in the state and output space are considered and other cases are in principle also possible. Furthermore, here the MPC is based on transformed system coordinates.

In recent years, the stabilization of one-dimensional manifolds or curves has gained more and more interest. In this context, the curves are usually called paths and therefore the corresponding control scheme is often named path following control. Trajectory tracking control also deals with the stabilization of curves. However, there the curves are equipped with a time-parameterization which turns them into trajectories. In contrast, for path following control no a priori time-parameterization of the curves is given. It has to be

inherently determined by the path following controller. The paths are typically defined in the output ([14], [29]) or state space ([15], [36], [38]) of a dynamical system. Path following control is closely related to manifold stabilization as a path can be seen as a one-dimensional manifold, see, e.g., [36] where this fact is used for controller design. Therefore, path following control is included in the framework presented in this paper as a special case. Nevertheless, there are many works in literature focusing on path following control based on different control approaches and tailored to different applications.

If the paths are given in the output space of the system, the corresponding zero path error manifold in the state space can be calculated and stabilized. This is done, e.g., in [11] for a unicycle and special types of paths. An interesting point in this work is the existence of a control law such that saturation constraints for the inputs can be considered. The same approach of determining and stabilizing the zero path error manifold is employed, e.g., in [1], [27], [29]. There, the invariance property is fulfilled but system constraints are not taken into account.

Other approaches to path following control are given by hybrid control strategies as well as Lyapunov and backstepping techniques, see, e.g., [8], [13], [35]. The utilization of MPC for path following control is investigated, e.g., in [14], [24], [38]. Real-time capable MPC schemes for path following are presented, e.g., in [5], [24]. MPC offers the possibility to systematically account for system constraints. However, often the invariance property is not fulfilled.

In summary, a controller for manifold stabilization or path following is expected to not only stabilize the respective manifold or path but it ideally also ensures the invariance property and a desired tangential movement. Moreover, usually system constraints have to be respected. Particularly in view of these constraints, a prioritization of the movement to the manifold over the tangential movement is of interest as well. To the best of the authors' knowledge, no other existing control scheme in literature for manifold stabilization and path following is able to simultaneously and systematically account for all these issues. The research presented in this paper aims at closing this gap. To this end, a novel tailored MPC scheme is proposed which relies on existing concepts of manifold stabilization transforming the original system description into coordinates of a TNF. Therefore, this work is also an extension of [4]. Depending on the underlying concept, manifolds in the state and output space can inter alia be considered. The existing approaches for the transformation to TNF do not consider system constraints. The extension with MPC presented in this paper allows to systematically incorporate such constraints. Furthermore, in contrast to other MPC approaches to manifold stabilization and path following in literature, the proposed MPC structure achieves the

above mentioned prioritization of the movement to the manifold over the tangential movement. Reaching the manifold is the primary target and no compromise between convergence to the manifold and movement on the manifold has to be taken. For practical applications, the prioritization is regarded important because imposing a desired tangential movement generally does not make sense if the manifold or path is not reached. On the other hand, it is essential for ensuring the invariance property under due consideration of the system constraints which is often not guaranteed by existing classical MPC schemes in literature. For these schemes, if the constraints are used to full capacity, usually a compromise situation occurs. In general, it provokes that the manifold or path is left and, hence, the invariance property is not fulfilled. Besides remedying this issue, the presented scheme allows to independently tune the convergence to the manifold and the movement on the manifold, which constitutes another difference to existing MPC approaches in literature.

This work is organized as follows. In Section 2 the TNFs are introduced which serve as the basis for the proposed MPC framework. The considered problem is stated in Section 3. Section 4 introduces the MPC scheme and in Section 5 its convergence properties are investigated. The theoretical results are applied to an illustrative example in Section 6 and some conclusions are drawn in Section 7.

Notation

The class \mathcal{K} contains all continuous, strictly increasing functions $\sigma : \mathbb{R}_{\geq 0} \rightarrow \mathbb{R}_{\geq 0}$ with $\sigma(0) = 0$ (cf. [31]). In the context of an OCP, the optimal quantities are indicated with the superscript $*$. All quantities in an OCP belonging to an MPC scheme are marked with a bar to clearly distinguish them from the actual quantities in the closed-loop system. The total derivatives of a function $x(t)$ with respect to time are denoted by \dot{x} , \ddot{x} , $x^{(3)}$, and so forth. Given a vector $y \in \mathbb{R}^n$, $\left(y\right)_Q$ represents the quadratic form $y^T Q y$ with the positive (semi-)definite matrix $Q \in \mathbb{R}^{n \times n}$. The index i refers to the i th component of the respective quantity. A diagonal matrix D with $D_{i,i} = y_i$ is denoted as $\text{diag}(y)$.

2 Transverse normal forms

The systems under consideration are given by

$$\begin{aligned}\dot{x} &= f(x, u) & (1a) \\ y &= h(x) & (1b)\end{aligned}$$

including the control-affine form

$$\begin{aligned}\dot{x} &= f(x) + g(x)u & (2a) \\ y &= h(x) & (2b)\end{aligned}$$

with state $x \in \mathbb{R}^n$, input $u \in \mathbb{R}^m$, and output $y \in \mathbb{R}^m$.

The MPC scheme for manifold stabilization presented in this paper relies on existing approaches which transform the original system description into a TNF with respect to the target manifold (the manifold to be stabilized). These target manifolds can be defined in different ways. Two possibilities are manifolds in the state space or output space of the system. The method of choice for transforming the original system description into a TNF depends amongst others on the properties of the system. A thorough treatment of all possible cases would go beyond the scope of this paper. Therefore, the subsequent investigations consider two common cases which are introduced in the following. Nevertheless, the control framework presented in Section 4 can in principle be extended to other cases as well.

2.1 Controlled invariant manifolds in the state space

In this section, results for the stabilization of controlled invariant submanifolds \mathcal{M}_s of the state space of control-affine dynamical systems (2a) are shortly repeated. Nielsen et al. give necessary and sufficient conditions in [30] for the existence of output functions with a well-defined relative degree allowing to perform input-output feedback linearization yielding the TNF, see also [20]. These output functions are representative for the off-the-manifold movement. Furthermore, the associated zero dynamics has to have the same dimension as \mathcal{M}_s . We consider systems and manifolds for which these conditions are satisfied. Following [30] the input transformation

$$u = \alpha(x) + \beta(x) \begin{bmatrix} v^{\text{h}} \\ v^{\text{l}} \end{bmatrix} \quad (3a)$$

and the invertible state transformation

$$\begin{bmatrix} \xi^{\text{T}} & \eta^{\text{T}} \end{bmatrix}^{\text{T}} = \Phi(x) \quad (3b)$$

transform the original system (2a) to TNF

$$\dot{\xi} = A^{\text{h}}\xi + B^{\text{h}}v^{\text{h}} \quad (4a)$$

$$\dot{\eta} = f^0(\eta, \xi) + g^{\text{h}}(\eta, \xi)v^{\text{h}} + g^{\text{l}}(\eta, \xi)v^{\text{l}} \quad (4b)$$

with the property

$$\Phi(\mathcal{M}_s) = \{(\xi, \eta) \mid \xi = 0\} \quad (5)$$

and (4a) being controllable. Due to (5) the system (4a) represents the transversal dynamics with corresponding state ξ , input v^{h} , and constant matrices A^{h} and B^{h} . Accordingly, the tangential dynamics characterizing the movement on \mathcal{M}_s are given by (4b) with state η and

input v^\parallel . In the following, the target manifold $\mathcal{M} = \Phi(\mathcal{M}_s)$ is expressed in the transformed coordinates in the form (5).

By inserting $x = \Phi^{-1}(\xi, \eta)$, which exists at least locally, into (3a) the input transformation in terms of the new coordinates of the TNF can be obtained. For a given initial condition $x(t_0) = x_0$ of system (2a), the initial conditions for the transformed coordinates directly follow from (3b)

$$\begin{bmatrix} \xi_0 \\ \eta_0 \end{bmatrix} = \Phi(x_0). \quad (6)$$

2.2 Manifolds in a flat output space

As opposed to Section 2.1, here the derivation of a TNF for manifolds \mathcal{M}_f in flat output spaces is described. To this end, the results given in [4] are shortly revisited. For a system (1) with y being a flat output, the manifold \mathcal{M}_f to be stabilized is defined as

$$\mathcal{M}_f = \{y \in \mathbb{R}^m \mid \sigma^\flat(y) = 0\} \quad (7)$$

with a continuous function $\sigma^\flat : \mathbb{R}^m \rightarrow \mathbb{R}^{m-p}$, $0 \leq p \leq m-1$, i.e., the manifold \mathcal{M}_f has dimension p . As outlined in [4] it is convenient to take another function of the flat outputs

$$\sigma^\parallel(y) : \mathbb{R}^m \rightarrow \mathbb{R}^p \quad (8)$$

into account. Under certain sufficient conditions given in [4] this allows to define a new flat output

$$z = \begin{bmatrix} y^\flat \\ y^\parallel \end{bmatrix} = \begin{bmatrix} \sigma^\flat(h(x)) \\ \sigma^\parallel(h(x)) \end{bmatrix} =: \Upsilon(x). \quad (9)$$

Based on (9) quasi-static exact linearization [9] can be carried out yielding the corresponding Brunovský normal form

$$y_i^{\flat(\hat{\rho}_i)} = \tilde{v}_i^\flat, \quad i = 1, \dots, m-p \quad (10a)$$

$$y_j^{\parallel(\hat{\rho}_j)} = \tilde{v}_j^\parallel, \quad j = 1, \dots, p. \quad (10b)$$

The Brunovský state belonging to (10) is given by

$$\tilde{\zeta}^\text{T} = \begin{bmatrix} \tilde{\zeta}^\text{T} & \tilde{\eta}^\text{T} \end{bmatrix} \quad (11)$$

with

$$\tilde{\zeta}^\text{T} = \begin{bmatrix} y_1^\flat & \dots & y_1^{\flat(\hat{\rho}_1-1)} & \dots & y_{m-p}^\flat & \dots & y_{m-p}^{\flat(\hat{\rho}_{m-p}-1)} \end{bmatrix} \quad (12a)$$

$$\tilde{\eta}^\text{T} = \begin{bmatrix} y_1^\parallel & \dots & y_1^{\parallel(\hat{\rho}_1-1)} & \dots & y_p^\parallel & \dots & y_p^{\parallel(\hat{\rho}_p-1)} \end{bmatrix}. \quad (12b)$$

The quasi-static state feedback [9] yielding (10) follows as

$$u = \tilde{\kappa} \left(\tilde{\zeta}, \tilde{v}^\flat, \dot{\tilde{v}}^\flat, \ddot{\tilde{v}}^\flat, \dots, \tilde{v}^\parallel, \dot{\tilde{v}}^\parallel, \ddot{\tilde{v}}^\parallel, \dots \right) \quad (13)$$

and the generalized state transformation linking x with $\tilde{\zeta}$ in general form reads as

$$x = \Lambda \left(\tilde{\zeta}, \tilde{v}^\flat, \dot{\tilde{v}}^\flat, \ddot{\tilde{v}}^\flat, \dots, \tilde{v}^\parallel, \dot{\tilde{v}}^\parallel, \ddot{\tilde{v}}^\parallel, \dots \right) \quad (14)$$

with $\tilde{v}^\flat = [\tilde{v}_1^\flat \dots \tilde{v}_{m-p}^\flat]^\text{T}$ and $\tilde{v}^\parallel = [\tilde{v}_1^\parallel \dots \tilde{v}_p^\parallel]^\text{T}$. In many cases, the inverse mappings

$$\tilde{\xi} = \bar{\Lambda}_1 \left(x, \tilde{v}^\flat, \dot{\tilde{v}}^\flat, \ddot{\tilde{v}}^\flat, \dots, \tilde{v}^\parallel, \dot{\tilde{v}}^\parallel, \ddot{\tilde{v}}^\parallel, \dots \right) \quad (15a)$$

$$\tilde{\eta} = \bar{\Lambda}_2 \left(x, \tilde{v}^\flat, \dot{\tilde{v}}^\flat, \ddot{\tilde{v}}^\flat, \dots, \tilde{v}^\parallel, \dot{\tilde{v}}^\parallel, \ddot{\tilde{v}}^\parallel, \dots \right) \quad (15b)$$

are explicitly available too. In the following, dynamic extension in the form of simple integrators is performed for each component of the new inputs \tilde{v}^\flat and \tilde{v}^\parallel by equating the highest derivative of \tilde{v}_i^\flat , $i = 1, \dots, m-p$, and \tilde{v}_j^\parallel , $j = 1, \dots, p$, in (13) with new inputs v_i^\flat and v_j^\parallel , respectively. The integrator states ζ_I are combined with $\tilde{\xi}$ and $\tilde{\eta}$ to the overall states of the TNF ξ and η . Thus, (13) can be written as

$$u = \kappa \left(\xi, \eta, v^\flat, v^\parallel \right) \quad (16)$$

with $v^\flat = [v_1^\flat \dots v_{m-p}^\flat]^\text{T}$ and $v^\parallel = [v_1^\parallel \dots v_p^\parallel]^\text{T}$. The dynamics in TNF are linear, time invariant, and controllable and can be stated as

$$\dot{\xi} = A^\flat \xi + B^\flat v^\flat \quad (17a)$$

$$\dot{\eta} = A^\parallel \eta + B^\parallel v^\parallel \quad (17b)$$

with the transverse and tangential dynamics (17a) and (17b). At time t_0 , one has the degree of freedom of choosing the initial conditions for the integrator states $\zeta_I(t_0)$. Therefore, together with x_0 , $\tilde{\xi}(t_0)$ and $\tilde{\eta}(t_0)$ can be calculated from (15). These quantities can be combined with $\zeta_I(t_0)$ yielding the overall mapping

$$(x_0, \zeta_I(t_0)) \rightarrow \begin{bmatrix} \xi_0 \\ \eta_0 \end{bmatrix}. \quad (18)$$

Remark 1 Here it is assumed that the highest derivatives of \tilde{v}_i^\flat , $i = 1, \dots, m-p$, and \tilde{v}_j^\parallel , $j = 1, \dots, p$ do not appear in (15). Therefore, only the integrator states $\zeta_I(t_0)$ are needed (besides x_0) to calculate (18).

In view of the dynamics (17) it is convenient to consider stabilization of the controlled invariant [20] manifold $\mathcal{M} = \{(\xi, \eta) \mid \xi = 0\}$ in the (extended) state space.

Stabilizing \mathcal{M} is equivalent to the stabilization of \mathcal{M}_f . Therefore, \mathcal{M} is also referred to as the target manifold in this case.

2.3 Summary

By comparing the results presented in Sections 2.1 and 2.2 it can be concluded that both presented manifold stabilization tasks can be covered by a TNF of the form (4) and a feedback law of the form (16). This setup is used as a basis for the subsequent investigations. Let $\Phi_t^\eta(\eta_k, \xi_k, v^\parallel(\cdot), v^\pitchfork(\cdot))$ denote the solution of (4b) and $\Phi_t^\xi(\xi_k, v^\pitchfork(\cdot)) = e^{A^\pitchfork(t-t_k)}\xi_k + \int_{t_k}^t e^{A^\pitchfork(t-t_k-\tau)}B^\pitchfork v^\pitchfork(\tau) d\tau$ the solution of (4a) for $t \geq t_k$ and initial values $\xi(t_k) = \xi_k, \eta(t_k) = \eta_k$.

In both cases, the goal of any controller is to asymptotically stabilize the origin of the transverse dynamics and thus stabilize the target manifold \mathcal{M} . The norm $\|\xi\|$ yields a measure of how far the system is away from the target manifold \mathcal{M} . By choosing $v^\pitchfork \equiv 0$ one can ensure that for $\xi = 0$ the system stays on the target manifold for all future times.

Due to the nonlinear nature of the system dynamics and the manifolds, the transformations and feedback laws together with the resulting TNFs might only exist locally. Therefore, it is assumed in the following that all those quantities exist in the whole region of interest or that this region can be covered by combining several local charts.

3 Problem statement

This section is devoted to defining the considered problem of manifold stabilization with input constraints by stating the control objectives. For this, it is assumed that the input u of (1) or (2) is subject to the input constraints $u(t) \in \mathcal{U}$. Furthermore, let us suppose that a TNF according to Section 2 can be derived for the manifold to be stabilized. Therefore, the control objectives can be directly formulated in terms of the transverse and tangential coordinates ξ and η :

- O1) Asymptotic convergence to the target manifold: This objective can be mathematically formulated as $\lim_{t \rightarrow \infty} \xi(t) = 0$. It implies that, for example, the state or output of the system approach the respective manifold to be stabilized.
- O2) Invariance property: If $\xi = 0$ holds at initial time t_0 , then $\xi(t) = 0$ has to be fulfilled for all $t \geq t_0$. This means that, e.g., the state or output of the system never leave the respective manifold again and it is rendered invariant.
- O3) Achieve a desired tangential movement on the manifold: In the coordinates of the TNF, this boils down to influencing the tangential dynamics with coordinates η in a desired way.

Remark 2 The target manifold \mathcal{M} is controlled invariant per construction based on the TNF. If O1) is achieved in such a way that the origin $\xi = 0$ of the transverse dynamics is rendered asymptotically stable, then the invariance property O2) is automatically fulfilled. As O1) is just formulated with convergence here, O2) is stated separately.

Remark 3 It is assumed that O1)–O3) can in principle be fulfilled in consideration of the input constraints.

Remark 4 In principle, constraints concerning the state x of (1) or (2), for example in the form $x(t) \in \mathcal{X}$, can also be considered with the presented scheme. Moreover, even mixed state and input constraints can be taken into account. However, the focus of this paper lies on the control scheme itself. Due to this fact and to enhance the clarity and readability, just input constraints are considered in this work. Nevertheless, the corresponding extensions for state constraints are straightforward.

4 Model predictive control scheme

The concepts introduced in Section 2 allow to calculate a TNF for a given manifold. However, a suitable control strategy is necessary in order to achieve the objectives stated in Section 3. In particular, the concepts of Section 2 do not allow the straightforward consideration of constraints. To this end, a tailored MPC scheme is proposed in the following. As usual, the proposed MPC scheme is based on a sampled-data strategy, see, e.g., [17]. This means that the system state is obtained at discrete sampling instants $t_k = kT_s$ with sampling time T_s . However, it is assumed that the optimal input can be applied in continuous-time fashion over the interval $[t_k, t_k + T_s)$.

Usually, MPC schemes rely on solving a *single* OCP per sampling instant. In contrast to that, the proposed scheme for manifold stabilization consists of solving *two* OCPs sequentially at each sampling instant, subsequently referred to as OCP1 and OCP2. The reasons for choosing this special structure are manifold and will be explained in more detail after defining the OCPs. The length of the optimization horizon is the same for both OCPs and will be denoted by T . The current optimization horizon at sampling instant t_k is termed $\mathcal{H}_k = [t_k, t_k + T]$. The initial conditions in both OCPs are given by $\bar{\xi}(t_k) = \xi_k$ and $\bar{\eta}(t_k) = \eta_k$ with ξ_k and η_k following from (6) or (18) for the system state x_k at sampling instant t_k . At every sampling instant t_k OCP1 is solved first with the TNF (4) and the feedback law

(16), see Section 2.3. It reads as

$$\min_{\bar{v}^{\hat{n}}(\cdot), \bar{v}^{\parallel}(\cdot)} J^{\hat{n}}(t_k, \bar{v}^{\hat{n}}(\cdot)) \quad (19a)$$

$$\text{s.t.} \quad \dot{\bar{\xi}} = A^{\hat{n}} \bar{\xi} + B^{\hat{n}} \bar{v}^{\hat{n}} \quad (19b)$$

$$\dot{\bar{\eta}} = f^0(\bar{\eta}, \bar{\xi}) + g^{\hat{n}}(\bar{\eta}, \bar{\xi}) \bar{v}^{\hat{n}} + g^{\parallel}(\bar{\eta}, \bar{\xi}) \bar{v}^{\parallel} \quad (19c)$$

$$\bar{\xi}(t_k + T) \in \mathcal{T}_1 \quad (19d)$$

$$\bar{\eta}(t_k + T) \in \mathcal{T}_2 \quad (19e)$$

$$\kappa(\bar{\xi}(t), \bar{\eta}(t), \bar{v}^{\hat{n}}(t), \bar{v}^{\parallel}(t)) \in \mathcal{U} \quad \forall t \in \mathcal{H}_k \quad (19f)$$

with the cost functional

$$J^{\hat{n}}(t_k, \bar{v}^{\hat{n}}(\cdot)) = \int_{t_k}^{t_k+T} l^{\hat{n}}(\xi(t), v^{\hat{n}}(t)) dt + V^{\hat{n}}(\xi(t_k + T)). \quad (20)$$

After solving OCP1, OCP2 is solved based on the optimal solution $\bar{\xi}^{1*}$, $\bar{\eta}^{1*}$, $\bar{v}^{\hat{n}1*}$, and $\bar{v}^{\parallel 1*}$ from OCP1. Since the optimal solutions for ξ and $v^{\hat{n}}$ are fixed by OCP1, they will henceforth be referred to as $\bar{\xi}^* = \bar{\xi}^{1*}$ and $\bar{v}^{\hat{n}*} = \bar{v}^{\hat{n}1*}$. OCP2 is defined as

$$\min_{\bar{v}^{\parallel}(\cdot)} J^{\parallel}(t_k, \bar{v}^{\parallel}(\cdot)) \quad (21a)$$

$$\text{s.t.} \quad \dot{\bar{\eta}} = f^0(\bar{\eta}, \bar{\xi}^*) + g^{\hat{n}}(\bar{\eta}, \bar{\xi}^*) \bar{v}^{\hat{n}*} + g^{\parallel}(\bar{\eta}, \bar{\xi}^*) \bar{v}^{\parallel} \quad (21b)$$

$$\bar{\eta}(t_k + T) \in \mathcal{T}_2 \quad (21c)$$

$$\kappa(\bar{\xi}^*(t), \bar{\eta}(t), \bar{v}^{\hat{n}*}(t), \bar{v}^{\parallel}(t)) \in \mathcal{U} \quad \forall t \in \mathcal{H}_k \quad (21d)$$

with the cost functional

$$J^{\parallel}(t_k, \bar{v}^{\parallel}(\cdot)) = \int_{t_k}^{t_k+T} l^{\parallel}(\eta(t), v^{\parallel}(t)) dt + V^{\parallel}(\eta(t_k + T)). \quad (22)$$

It is assumed that a solution to both OCPs exists for appropriate initial conditions. Terminal constraints are included in both OCPs with the sets \mathcal{T}_1 and \mathcal{T}_2 . Further details regarding these sets and the required properties of the cost functionals are given in Section 5.

OCP1 is dedicated to the movement transverse to the target manifold whereas OCP2 is responsible for the tangential movement. The desired properties of the transverse movement can be shaped with $J^{\hat{n}}$ and those of the tangential movement with J^{\parallel} . A reasonable choice for the integral cost function and the terminal cost in $J^{\hat{n}}$ is

given by

$$l^{\hat{n}}(\xi, v^{\hat{n}}) = \frac{1}{2} \left(\left(\xi \right)_{Q_{\xi}} + \left(v^{\hat{n}} \right)_{R^{\hat{n}}} \right) \quad (23a)$$

$$V^{\hat{n}}(\xi) = \frac{1}{2} \left(\xi \right)_{S_{\xi}}, \quad (23b)$$

with the positive (semi-)definite weighting matrices Q_{ξ} , $R^{\hat{n}}$, and S_{ξ} . Due to the fact that the desired tangential movement heavily depends on the application at hand, the integral cost function l^{\parallel} and the terminal cost V^{\parallel} are not specified at this point. As already mentioned before, OCP1 yields $\bar{\xi}^*$ and $\bar{v}^{\hat{n}*}$. Moreover, it is necessary to solve for $\bar{\eta}$ and \bar{v}^{\parallel} as well because the feedback law for u is in general depending on these quantities. However, the final result $\bar{\eta}^*$ and $\bar{v}^{\parallel*}$ is determined in OCP2. The transverse and tangential inputs in the closed-loop system are given by

$$v^{\hat{n}*}(t) = \bar{v}^{\hat{n}*}(t), \quad t \in [t_k, t_k + T_s] \quad (24a)$$

$$v^{\parallel*}(t) = \bar{v}^{\parallel*}(t), \quad t \in [t_k, t_k + T_s]. \quad (24b)$$

The corresponding state trajectories in the closed-loop system are denoted by ξ^* and η^* and the actual input applied to the system is given by

$$u(t) = \kappa(\xi^*(t), \eta^*(t), v^{\hat{n}*}(t), v^{\parallel*}(t)), \quad t \geq t_0. \quad (25)$$

The verification that the objectives defined in Section 3 are fulfilled is postponed to the proof of Theorem 16.

The most important motivation for choosing the structure with two OCPs is given by the invariance property O2). Many existing model predictive control concepts from literature with just one OCP (e.g., [15], [24]) suffer from a compromise between terms in the cost functional weighting the transverse and the tangential movement. To be more specific, it may happen that an increase in the value of the cost functional due to leaving the target manifold can be counterbalanced with a better performance in tangential direction. This case cannot occur with the proposed strategy as the transverse movement is determined in OCP1 solely based on the transverse cost functional $J^{\hat{n}}$.

Another reason for choosing two OCPs is that the movement to the manifold O1) is prioritized over the tangential movement O3). The prioritization arises from the fact that the quantities $\bar{\xi}^*$ and $\bar{v}^{\hat{n}*}$ are determined first in OCP1 and influence the tangential dynamics in (21b). Furthermore, it is related to the input constraints. OCP1 has the possibility to utilize the system inputs u up to their limits for minimizing $J^{\hat{n}}$. Roughly speaking, any remaining margin in the control input u can be used by OCP2 for the tangential movement. If there is no margin left, OCP2 cannot influence the desired tangential

movement which will also be illustrated with the example in Section 6. The prioritization is a useful feature as imposing a desired tangential movement is useless if the system does not move toward the target manifold. Furthermore, the coordinates η might not be meaningful unless the system is in a vicinity of the target manifold.

A further benefit of utilizing two OCPs is that the desired properties of the movement to the target manifold and the tangential movement can be chosen independently of each other. This is possible by the decoupled cost functionals in OCP1 and OCP2. For existing approaches in the literature relying on a single OCP, again a compromise has to be made in this respect.

Remark 5 *In general it is possible that the tangential dynamics cannot be influenced, i.e., there are no control inputs v^\parallel . This may happen, e.g., for the framework presented in Section 2.1. In this case, it does not make any sense to define a desired movement on the manifold and OCP2 is superfluous. The consideration of OCP1 is sufficient in order to calculate the original inputs u for the system.*

Remark 6 *Other manifolds or systems can in principle be considered as well provided that a TNF similar to the ones shown in Section 2 can be derived. In these cases, the structures of OCP1 and OCP2 remain the same. The things that possibly change are the structure of the system equations (19b), (19c), and (21b) as well as the feedback laws (19f) and (21d) for incorporating the input constraints. However, the setup with two sequentially solved OCPs in this form heavily relies on the fact that the transverse dynamics are decoupled from the tangential dynamics. Therefore, the presented framework is limited to TNFs possessing this property.*

5 Investigation of convergence

In this section, one particular method is chosen for proving convergence of the proposed MPC scheme. Several assumptions concerning the optimal solutions and the weighting functions of (19) and (21) as well as the system equations are necessary for a rigorous mathematical proof of convergence. In addition, it is convenient to slightly restrict the structure of l^\parallel .

Assumption 7 *The optimal solutions of (19) and (21) are such that $\|\xi^*(t)\| \leq \varepsilon_\xi$ and $\|\bar{\eta}^*(t)\| \leq \varepsilon_\eta \forall t \in \mathcal{H}_k$ with $k = 0, 1, 2, \dots$ and finite $\varepsilon_\xi, \varepsilon_\eta \in \mathbb{R}_{>0}$, i.e., $\bar{\xi}^*(t)$ and $\bar{\eta}^*(t)$ are contained in the compact sets $\mathcal{Y}_k = \{\xi \mid \|\xi\| \leq \varepsilon_\xi\}$ and $\mathcal{Z}_k = \{\eta \mid \|\eta\| \leq \varepsilon_\eta\}$ for all $t \in \mathcal{H}_k$. Furthermore, the optimal inputs $\bar{v}^{\parallel*}$ and $\bar{v}^{\perp*}$ are supposed to be bounded.*

Remark 8 *Assumption 7 as well as the following ones are mainly of technical nature and might be modified or*

even dropped if a different approach for the proof of convergence is employed, see, e.g., [16], [21], [32]. The assumption of a bounded tangential state is not restrictive at all as it can usually be achieved by a suitable choice of η .

Assumption 9 *The functions $f^0(\eta, \xi)$, $g^\perp(\eta, \xi)$, and $g^\parallel(\eta, \xi)$ are continuous for all $(\eta, \xi) \in \mathcal{Z}_k \times \mathcal{Y}_k$, $k \in \{0, 1, 2, \dots\}$.*

Assumption 10 *The integral cost function l^\perp is bounded from below with a class \mathcal{K} function λ_l^\perp in the form*

$$\lambda_l^\perp(\|\xi\|) \leq l^\perp(\xi, v^\perp) \quad (26)$$

and $l^\perp(0, 0) = 0$ holds.

Assumption 11 *The integral cost function l^\parallel can be written in the form $l^\parallel(\eta, v^\parallel) = l_\eta^\parallel(\eta) + l_v^\parallel(v^\parallel) \geq l_\eta^\parallel(\eta)$ with a continuous function $l_\eta^\parallel(\eta) \geq 0 \forall \eta$ and a function $l_v^\parallel(v^\parallel) \geq 0 \forall v^\parallel$. Moreover, l_η^\parallel is such that for $l_\eta^\parallel = 0$, the desired tangential movement is achieved.*

Assumption 12 *The terminal costs V^\perp and V^\parallel are continuously differentiable and V^\perp is positive definite.*

Remark 13 *The Assumptions 10 and 12 (concerning V^\perp) are fulfilled with (23) and choosing Q_ξ , R^\perp , and S_ξ positive definite.*

The main idea for enforcing convergence is to use the terminal set \mathcal{T}_1 in a way that it represents a neighborhood of the target manifold \mathcal{M} which is defined as

$$\Omega_{\mathcal{M}}^\varepsilon = \{\xi \mid V^\perp(\xi) \leq \varepsilon\} = \mathcal{T}_1 \quad (27)$$

with $\varepsilon \in \mathbb{R}_{>0}$. Let \mathcal{N} be the set of all η which are required in order to achieve the desired tangential movement (containing, e.g., a desired target point on \mathcal{M}). Additionally, $\mathcal{N}' = \{(\xi, \eta) \mid \xi = 0, \eta \in \mathcal{N}\} \subset \mathcal{M}$ is defined.

Assumption 14 *There exist input functions $v_T^\perp(t)$ and $v_T^\parallel(t)$ for $t \in [0, T_s]$ such that for every point $(\xi_n, \eta_n) \in \Omega_{\mathcal{M}}^\varepsilon \times \mathcal{N}$ it holds $\forall t \in [0, T_s]$ that*

$$\kappa\left(\xi_T(t), \eta_T(t), v_T^\perp(t), v_T^\parallel(t)\right) \in \mathcal{U} \quad (28)$$

and

$$\frac{d}{dt}\left(V^\perp(\xi_T(t))\right) + l^\perp(\xi_T(t), v_T^\perp(t)) \leq 0 \quad (29a)$$

$$\frac{d}{dt}\left(V^\parallel(\eta_T(t))\right) + l^\parallel(\eta_T(t), v_T^\parallel(t)) \leq 0 \quad (29b)$$

with (see Section 2.3)

$$\xi_T(t) := \Phi_t^\xi(\xi_n, v_T^{\hat{\eta}}(\cdot)) \quad (30a)$$

$$\eta_T(t) := \Phi_t^\eta(\eta_n, \xi_n, v_T^{\hat{\eta}}(\cdot), v_T^{\hat{\eta}}(\cdot)) \in \mathcal{N}. \quad (30b)$$

The requirements (28) and (29) arise in a natural way for the considered task described in Section 3. The condition (28) demands that in a vicinity of the manifold expressed by $\Omega_{\mathcal{M}}^\varepsilon$ input functions do exist in principle for driving the system under due consideration of the constraints. The condition (29a) mainly expresses the desire that the input functions $v_T^{\hat{\eta}}$ have to move the system toward the target manifold. The input functions v_T^{\parallel} have to ensure that the application-specific requirements for movement on the manifold are fulfilled which is indirectly stated in (29b). While meeting these requirements it is necessary that η does not leave the (feasible) set \mathcal{N} which is expressed by (30b). All these requirements arise naturally from the considered task. If they are not accomplishable, the considered task is not feasible.

What might be restricting is the expression of the requirements in terms of the terminal costs and integral cost terms in (29). However, this is just one possibility to prove convergence, other approaches do exist in literature, for example by utilizing a sufficiently long optimization horizon [21] or by relying on a controllability assumption [32]. However, the chosen way to prove convergence of the proposed MPC scheme is a common approach, see, e.g., [15], [17], [21].

Remark 15 *From the point of view of stabilizing the target manifold, it is clear that the input functions $v_T^{\hat{\eta}}$ have to exist in a vicinity $\Omega_{\mathcal{M}}^\varepsilon$ of the target manifold with $\varepsilon > 0$. Regarding the movement on the manifold (application-specific goals) the existence of v_T^{\parallel} for $\varepsilon = 0$ would in principle be sufficient.*

The following theorem states the main result with the terminal sets chosen as $\mathcal{T}_1 = \Omega_{\mathcal{M}}^\varepsilon$ and $\mathcal{T}_2 = \mathcal{N}$.

Theorem 16 *Consider the MPC scheme based on the sequential solution of the OCPs (19) and (21) with a sampling time T_s , an optimization horizon with length $T \geq T_s$, $\mathcal{T}_1 = \Omega_{\mathcal{M}}^\varepsilon$, and $\mathcal{T}_2 = \mathcal{N}$. Let the Assumptions 7, 9, 10, 11, 12, and 14 hold for a particular choice of ε . If the OCPs (19) and (21) have a feasible solution at time t_0 with ξ_0 and η_0 following from (6) or (18) and a particular choice of $\zeta_I(t_0)$ then*

- (1) the OCPs (19) and (21) have feasible solutions for all sampling instants t_k , $k > 0$,
- (2) the system state converges to the target manifold \mathcal{M} , i.e., O1 is achieved,
- (3) the invariance property O2) is accomplished,

- (4) O3) is fulfilled, i.e., the application-specific desired movement on the manifold is achieved for $t \rightarrow \infty$.

The region of attraction of the proposed MPC scheme is the set of all initial conditions x_0 for which a feasible solution of the OCPs (19) and (21) exists.

Proof. The proof relies on ideas presented, e.g., in [7], [17], [18], and [25]. While usually MPC schemes with one OCP per sampling instant are considered, here the optimal solutions of two OCPs per sampling instant have to be determined. For the ease of notation, let $\bar{v}^{\hat{\eta}*}$ and $\bar{v}^{\parallel*}$ denote the optimal solution of (19) and (21), respectively, at a generic sampling instant t_k . The value function of both OCPs (19) and (21) together is defined as $W(t_k) = J^{\hat{\eta}}(t_k, \bar{v}^{\hat{\eta}*}(\cdot)) + J^{\parallel}(t_k, \bar{v}^{\parallel*}(\cdot))$. Since neither disturbances nor model uncertainties are considered for the presented MPC scheme, the system state at any initial time $t_k + s$ with $s \in [0, T_s]$ follows as

$$\xi_s := \Phi_{t_k+s}^\xi(\xi_k, \bar{v}^{\hat{\eta}*}(\cdot)) \quad (31a)$$

$$\eta_s := \Phi_{t_k+s}^\eta(\eta_k, \xi_k, \bar{v}^{\parallel*}(\cdot), \bar{v}^{\hat{\eta}*}(\cdot)). \quad (31b)$$

Thus, $\bar{v}^{\hat{\eta}*}$ and $\bar{v}^{\parallel*}$ are feasible inputs on the time interval $[t_k + s, t_k + T]$. Furthermore, according to OCP1 and OCP2 ξ^* and $\bar{\eta}^*$ reach $\mathcal{T}_1 = \Omega_{\mathcal{M}}^\varepsilon$ and $\mathcal{T}_2 = \mathcal{N}$ at $t_k + T$. By combining these facts, feasible inputs for (19) and (21) at any time $t_k + s$ are given by

$$\hat{v}^{\hat{\eta}}(t) = \begin{cases} \bar{v}^{\hat{\eta}*}(t) & t \in [t_k + s, t_k + T] \\ v_T^{\hat{\eta}}(t - t_k - T) & t \in (t_k + T, t_k + s + T] \end{cases} \quad (32a)$$

$$\hat{v}^{\parallel}(t) = \begin{cases} \bar{v}^{\parallel*}(t) & t \in [t_k + s, t_k + T] \\ v_T^{\parallel}(t - t_k - T) & t \in (t_k + T, t_k + s + T]. \end{cases} \quad (32b)$$

The inputs $v_T^{\hat{\eta}}$ and v_T^{\parallel} follow according to Assumption 14 for $\eta_n = \Phi_{t_k+T}^\eta(\eta_k, \xi_k, \bar{v}^{\parallel*}(\cdot), \bar{v}^{\hat{\eta}*}(\cdot))$ and $\xi_n = \Phi_{t_k+T}^\xi(\xi_k, \bar{v}^{\hat{\eta}*}(\cdot))$. In particular, feasible inputs for (19) and (21) exist at the next sampling instant $t_{k+1} = t_k + T_s$. Thus, recursive feasibility (i.e., a feasible solution of (19) and (21) can be found at all sampling instants t_k , $k > 0$) is ensured due to the fact that per assumption (19) and (21) are solvable at time t_0 .

Let $\Phi_t^\xi(\xi_s, \hat{v}^{\hat{\eta}}(\cdot))$ and $\Phi_t^\eta(\eta_s, \xi_s, \hat{v}^{\parallel}(\cdot), \hat{v}^{\hat{\eta}}(\cdot))$ denote the solution of (4) with initial values ξ_s and η_s for $t_k + s$ and inputs $v^{\hat{\eta}} = \hat{v}^{\hat{\eta}}$, $v^{\parallel} = \hat{v}^{\parallel}$. For convenience, the shortcuts $\Phi_t^{\xi_s}$ and $\Phi_t^{\eta_s}$ will be used in the following for these solutions. It holds that $\Phi_{t_k+T}^{\xi_s} \in \Omega_{\mathcal{M}}^\varepsilon$ and $\Phi_{t_k+T}^{\eta_s} \in \mathcal{N}$.

At $t_k + s$ the value function fulfills

$$W(t_k + s) \leq J^{\text{h}}(t_k + s, \hat{v}^{\text{h}}(\cdot)) + J^{\text{l}}(t_k + s, \hat{v}^{\text{l}}(\cdot)). \quad (33)$$

Having in mind that $\bar{\eta}^*(t) = \Phi_t^{\eta}(\eta_k, \xi_k, \bar{v}^{\text{h}*}(\cdot), \bar{v}^{\text{l}*}(\cdot))$ and $\bar{\xi}^*(t) = \Phi_t^{\xi}(\xi_k, \bar{v}^{\text{h}*}(\cdot))$ and by proceeding along the lines of, e.g., [17], (33) can be expanded using (29) to

$$W(t_k + s) \leq J^{\text{h}}(t_k, \bar{v}^{\text{h}*}(\cdot)) + J^{\text{l}}(t_k, \bar{v}^{\text{l}*}(\cdot)) - \int_{t_k}^{t_k+s} l^{\text{h}}(\bar{\xi}^*(t), \bar{v}^{\text{h}*}(t)) dt - \int_{t_k}^{t_k+s} l^{\text{l}}(\bar{\eta}^*(t), \bar{v}^{\text{l}*}(t)) dt, \quad (34)$$

see Appendix A for some intermediate steps leading to (34). From (34) and by utilizing Assumptions 10 and 11 in the form

$$\int_{t_k}^{t_k+s} l^{\text{h}}(\bar{\xi}^*(t), \bar{v}^{\text{h}*}(t)) + l^{\text{l}}(\bar{\eta}^*(t), \bar{v}^{\text{l}*}(t)) dt \geq \int_{t_k}^{t_k+s} \lambda_l^{\text{h}}(\|\bar{\xi}^*(t)\|) + l_{\eta}^{\text{l}}(\bar{\eta}^*(t)) dt \quad (35)$$

it follows that

$$W(t_k + s) \leq W(t_k) - \int_{t_k}^{t_k+s} \lambda_l^{\text{h}}(\|\bar{\xi}^*(t)\|) + l_{\eta}^{\text{l}}(\bar{\eta}^*(t)) dt. \quad (36)$$

By induction it can be inferred that (it is assumed w.l.o.g. that $t_0 = 0$)

$$W(\infty) - W(0) \leq - \int_0^{\infty} \lambda_l^{\text{h}}(\|\xi^*(t)\|) + l_{\eta}^{\text{l}}(\eta^*(t)) dt. \quad (37)$$

Due to the fact that neither disturbances nor model uncertainties are considered and in view of Assumption 7 it follows that there exist compact sets \mathcal{Y} and \mathcal{Z} with the property $\xi^*(t) \in \mathcal{Y}$ and $\eta^*(t) \in \mathcal{Z}$ for all $t \geq 0$. This particularly entails that $\xi^*(t)$ and $\eta^*(t)$ are bounded which together with Assumptions 7 and 9 and the facts that (4a) is linear in ξ and v^{h} and (4b) is affine in v^{h} and v^{l} induces that $\dot{\xi}^*$ and $\dot{\eta}^*$ are bounded. Thus, $\xi^*(t)$ and $\eta^*(t)$ are uniformly continuous in t , see [10]. As every continuous function on a compact set is uniformly continuous it follows from Assumptions 10 and 11 that $\lambda_l^{\text{h}}(\cdot)$ and $l_{\eta}^{\text{l}}(\cdot)$ are uniformly continuous on \mathcal{Y} and \mathcal{Z} , respectively. Hence, from the fact that the composition of two uniformly continuous functions is again uniformly continuous and that every vector norm is continuous, the uniform continuity of $\lambda_l^{\text{h}}(\|\xi^*(t)\|)$ and $l_{\eta}^{\text{l}}(\eta^*(t))$ results.

Per assumption the OCPs (19) and (21) have a solution at t_0 which induces that $W(0)$ is bounded. Further-

more, $W(\infty) \geq 0$ which entails that $\int_0^{\infty} \lambda_l^{\text{h}}(\|\xi^*(t)\|) + l_{\eta}^{\text{l}}(\eta^*(t)) dt$ exists and is bounded. The upcoming final conclusions require the following lemma.

Lemma 17 (Barbalat's lemma, see [23]) Let $\Phi : \mathbb{R} \rightarrow \mathbb{R}$ be a uniformly continuous function on $[0, \infty)$.

Suppose that $\lim_{t \rightarrow \infty} \int_0^t \Phi(\tau) d\tau$ exists and is finite. Then, $\Phi(t) \rightarrow 0$ as $t \rightarrow \infty$.

By utilizing Lemma 17 together with the fact that $\lambda_l^{\text{h}}(\|\xi^*(t)\|)$ and $l_{\eta}^{\text{l}}(\eta^*(t))$ are uniformly continuous the conclusion

$$\lambda_l^{\text{h}}(\|\xi^*(t)\|) + l_{\eta}^{\text{l}}(\eta^*(t)) \rightarrow 0 \text{ for } t \rightarrow \infty \quad (38)$$

can be drawn which implies $\xi^*(t) \rightarrow 0$ and $l_{\eta}^{\text{l}} \rightarrow 0$. Hence, convergence to the target manifold \mathcal{M} is proven and, according to Assumption 11, the application-specific desired movement on the manifold is achieved for $t \rightarrow \infty$. This means that Objectives O1) and O3) are accomplished.

As pointed out, recursive feasibility is ensured for all sampling instants t_k , $k > 0$, provided that a feasible solution can be found at t_0 . Together with the proven convergence of the proposed scheme it follows that the region of attraction is the set of all initial conditions x_0 for which a feasible solution of the OCPs (19) and (21) exists.

The invariance property O2) is fulfilled in the application-relevant set \mathcal{N}' as for $\xi = 0$ and according to Assumption 14 the optimal solution $\bar{v}^{\text{h}*} \equiv 0$ of OCP1 is feasible and therefore ξ will remain zero. \square

One possible way for determining ε and all other degrees of freedom for a given application is pointed out in Section 6.

Remark 18 For the choice $\varepsilon = 0$ the terminal set reduces to the target manifold itself. This is a similar condition as in [14] where the usage of predictive control for path following is investigated.

6 Simulation example

A two-dimensional manifold is stabilized for a point-like mass moving in three-dimensional space. The states x_1 , x_3 , and x_5 are the coordinates in e_x , e_y , and e_z direction with e_i being the basis vectors of a Cartesian coordinate system and

$$x_2 = \dot{x}_1, \quad x_4 = \dot{x}_3, \quad x_6 = \dot{x}_5 \quad (39a)$$

are the corresponding velocities. Without loss of generality, the mass of the particle is supposed to be 1 and thus the remaining system equations read as

$$\dot{x}_2 = u_1, \dot{x}_4 = u_2, \dot{x}_6 = u_3 \quad (39b)$$

$$y = h(x) = \begin{bmatrix} x_1 & x_3 & x_5 \end{bmatrix}^T. \quad (39c)$$

The inputs u are given by the forces acting on the particle. They are subject to constraints $\mathcal{U} = \{u \in \mathbb{R}^3 | u_{\min} \leq u \leq u_{\max}\}$ with $u_{\max} = [0.1 \ 0.2 \ 0.9]^T$ and $u_{\min} = -u_{\max}$.

Remark 19 *Symmetric box constraints are considered here as they frequently occur for mechanical systems. However it is worth noting that asymmetric box constraints can be taken into account in a similar way.*

Obviously, y is a flat output of (39). Therefore, the method of Section 2.2 is applied here. The manifold \mathcal{M}_f to be stabilized with dimension $p = 2$ is defined in the flat output space by the function

$$\sigma^{\text{fl}}(y) = ay_2 + d \sin(cy_2) - y_3 \quad (40)$$

with $a = -1$, $c = 4$, and $d = 0.2$, see Fig. 1. As outlined in Section 2.2, another function σ^{\parallel} is chosen as

$$\sigma^{\parallel}(y) = \begin{bmatrix} y_1 & y_2 \end{bmatrix}^T. \quad (41)$$

It describes the position of the particle on \mathcal{M}_f . It can be easily verified that $\Upsilon(x) = [\Upsilon_1(x) \ \Upsilon_2(x) \ \Upsilon_3(x)]^T$ according to (9) is a new flat output allowing for an exact state linearization by static state feedback

$$u = \bar{\kappa}(x, v^{\text{fl}}, v^{\parallel}) = \alpha(x) + \beta(x) \begin{bmatrix} v^{\text{fl}} & v_1^{\parallel} & v_2^{\parallel} \end{bmatrix}^T. \quad (42)$$

The TNF follows with $\xi \in \mathbb{R}^2$ and $\eta \in \mathbb{R}^4$ as

$$\dot{\zeta} = \begin{bmatrix} \dot{\xi}^T & \dot{\eta}^T \end{bmatrix}^T = \begin{bmatrix} \xi_2 & v^{\text{fl}} & \eta_2 & v_1^{\parallel} & \eta_4 & v_2^{\parallel} \end{bmatrix}^T \quad (43)$$

and the corresponding state transformation is given by

$$\zeta = \Phi(x) = \begin{bmatrix} \Upsilon_1(x) & \dot{\Upsilon}_1(x) & x_1 & x_2 & x_3 & x_4 \end{bmatrix}^T \quad (44)$$

allowing to calculate

$$\kappa(\xi, \eta, v^{\text{fl}}, v^{\parallel}) = \bar{\kappa}(x, v^{\text{fl}}, v^{\parallel}) \Big|_{x=\Phi^{-1}(\zeta)}. \quad (45)$$

Thus, the controlled invariant target manifold expressed in the original coordinates x reads as

$$\mathcal{M} = \left\{ x \in \mathbb{R}^6 | \Upsilon_1(x) = \dot{\Upsilon}_1(x) = 0 \right\}. \quad (46)$$

For the considered application, Objective O3) is specified such that the particle approaches a desired point on the manifold which, for the sake of simplicity, is chosen as $\eta_d = 0$. Hence, the integral cost function and terminal cost for OCP2 are chosen as

$$l^{\parallel}(\eta, v^{\parallel}) = \frac{1}{2} \underbrace{\begin{pmatrix} \eta \end{pmatrix}_{Q_{\eta}}}_{l_{\eta}^{\parallel}(\eta)} + \frac{1}{2} \underbrace{\begin{pmatrix} v^{\parallel} \end{pmatrix}_{R^{\parallel}}}_{l_v^{\parallel}(v^{\parallel})} \quad (47a)$$

$$V^{\parallel}(\eta) = \frac{1}{2} \begin{pmatrix} \eta \end{pmatrix}_{S_{\eta}} \quad (47b)$$

with positive definite matrices Q_{η} , R^{\parallel} , and S_{η} . The corresponding terms for OCP1 are taken from (23) with positive definite weighting matrices Q_{ξ} , R^{fl} , and S_{ξ} . These choices entail that Assumptions 10, 11, and 12 are fulfilled. The set \mathcal{N} is expressed in terms of the terminal cost V^{\parallel} in the form

$$\mathcal{N} = \left\{ \eta \in \mathbb{R}^4 | V^{\parallel}(\eta) \leq N \right\} \quad (48)$$

with $N \in \mathbb{R}_{>0}$. The crucial part is given by finding feedback laws and suitable parameter values such that Assumption 14 is fulfilled. To this end, a strategy similar to the one proposed in, e.g., [6] is employed. The input functions v_T^{fl} and v_T^{\parallel} are chosen as linear state feedback laws which asymptotically stabilize the transverse and tangential dynamics. In the following, the derivation is explicitly stated for the transverse dynamics. With

$$v_T^{\text{fl}} = K^{\text{fl}} \xi \quad (49)$$

inserted for v^{fl} the transverse dynamics follow as

$$\dot{\xi} = \underbrace{\left(\begin{bmatrix} 0 & 1 \\ 0 & 0 \end{bmatrix} + \begin{bmatrix} 0 \\ 1 \end{bmatrix} K^{\text{fl}} \right)}_{A_c^{\text{fl}}} \xi. \quad (50)$$

Thus, when using (49) for v^{fl} the total derivative of V^{fl} with respect to time and the integral cost function read as

$$\dot{V}_T^{\text{fl}} = \frac{1}{2} \begin{pmatrix} \xi \end{pmatrix}_{A_c^{\text{fl}T} S_{\xi} + S_{\xi} A_c^{\text{fl}}} \quad (51a)$$

$$l_T^{\text{fl}} = \frac{1}{2} \begin{pmatrix} \xi \end{pmatrix}_{Q_{\xi} + K^{\text{fl}T} R^{\text{fl}} K^{\text{fl}}}. \quad (51b)$$

The determination of S_{ξ} as the solution of the Lyapunov equation

$$A_c^{\text{fl}T} S_{\xi} + S_{\xi} A_c^{\text{fl}} + \left(Q_{\xi} + K^{\text{fl}T} R^{\text{fl}} K^{\text{fl}} \right) = 0 \quad (52)$$

implies $\dot{V}_T^{\text{fl}} + l_T^{\text{fl}} = 0$ and hence (29a) holds. The strategy for the tangential dynamics is identical. Therefore,

(29b) is satisfied as well. Note that the condition (30b) is automatically fulfilled due to the expression of \mathcal{N} in terms of V^{\parallel} and $\dot{V}_T^{\parallel} \leq 0$.

Finally, ε and N are determined such that (28) is fulfilled. This is done by numerically searching for the maximum and minimum of each component of

$$\kappa \left(\xi, \eta, v^{\text{th}}, v^{\parallel} \right) \Big|_{v^{\text{th}}=K^{\text{th}}\xi, v^{\parallel}=K^{\parallel}\eta} \quad (53)$$

in the set $\Omega_{\mathcal{M}}^{\varepsilon} \times \mathcal{N}$. For $\varepsilon = 1$ and $N = 10$ the maxima and minima lie within the feasible region for the inputs. The other parameter values behind these results are

$$Q_{\xi} = \text{diag} \left(\begin{bmatrix} 1 & 1 \end{bmatrix} \right) \quad Q_{\eta} = \text{diag} \left(\begin{bmatrix} 1 & 1 & 8 & 8 \end{bmatrix} \right) \quad (54a)$$

$$R^{\text{th}} = 1 \quad R^{\parallel} = \text{diag} \left(\begin{bmatrix} 1 & 1 \end{bmatrix} \right) \quad (54b)$$

$$K^{\text{th}} = - \begin{bmatrix} 0.0016 & 0.08 \end{bmatrix} \quad K^{\parallel} = - \begin{bmatrix} 0.01 & 0.2 & 0 & 0 \\ 0 & 0 & 0.04 & 0.4 \end{bmatrix}. \quad (54c)$$

Hence, according to Theorem 16, the Objectives O1)–O3) are achieved for all x_0 for which feasible solutions of OCP1 and OCP2 exist. For the MPC scheme, a sampling time $T_s = 50\text{ms}$ together with an optimization horizon of length $T = 8\text{s}$ is chosen.

Unless otherwise stated, the simulation results shown in the following are based on the initial condition $x_0 = [0.1 \ 0.45 \ 2 \ 0 \ 0 \ -2]^T$ at $t_0 = 0$. Figure 1 shows the closed-loop trajectory of the particle in the three-dimensional space from two different viewpoints (solid line) with $y_0 = [x_{0,1} \ x_{0,3} \ x_{0,5}]^T$. The corresponding inputs (i.e., the forces acting on the particle) are depicted in Fig. 2. Obviously, the input constraints are frequently reached. The dashed trajectories in Fig. 1 belong to a few other initial conditions. From all starting points, the position of the particle asymptotically converges to the manifold \mathcal{M}_f . Furthermore, it also reaches the target position $y_d = 0$ (the origin of the Cartesian coordinate system). This illustrates that Objectives O1) and O3) are met. The dash-dot line in Fig. 1 traces the trajectory of the particle originating from $x_0 = [0.5 \ 0 \ 2 \ 0 \ 2a + d \sin(2c) \ 0]^T$ which corresponds to a position of rest exactly on \mathcal{M}_f . Again, the particle is driven to the desired target position $y_d = 0$ but never leaves \mathcal{M}_f again. This demonstrates the invariance property O2) achieved by the controller.

The transverse state ξ^* and the transverse control input $v^{\text{th}*}$ are visible in the left part of Fig. 3. As both transverse states converge to zero, the particle approaches the manifold. The value function of both OCPs over time

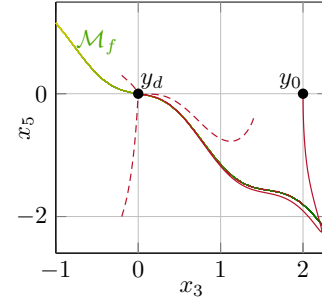
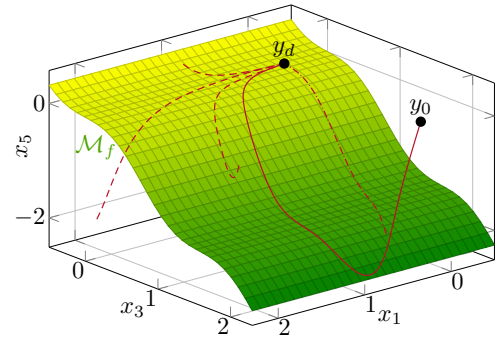


Fig. 1. Trajectories of the particle and \mathcal{M}_f .

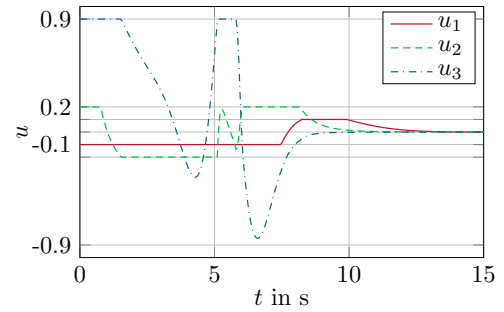


Fig. 2. System inputs u .

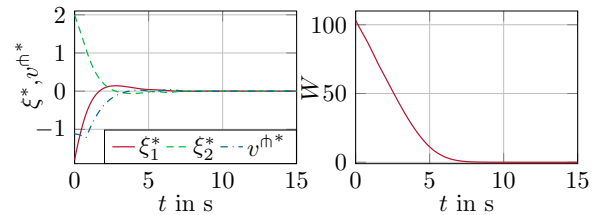


Fig. 3. Transverse state ξ^* , transverse control input $v^{\text{th}*}$, and combined value function W of both OCPs.

is shown in the right part of Fig. 3. As expected, W strictly decreases monotonically which practically verifies the convergence results of Section 5. In Fig. 4, the tangential state η^* and the corresponding control input $v^{\parallel*}$ are depicted. The convergence of all components of η^* to zero again verifies the fulfillment of Objective O3).

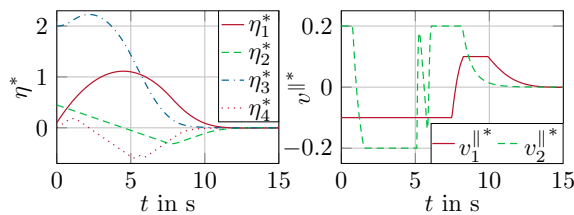


Fig. 4. Tangential state η^* and tangential control input $v^{\parallel*}$.

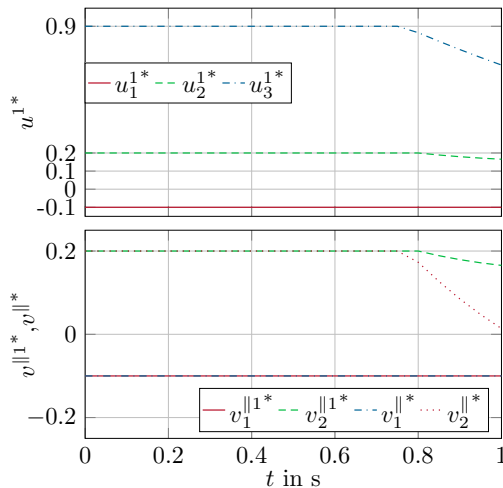


Fig. 5. Illustration of the prioritization property through u^{1*} , $v^{\parallel 1*}$, and $v^{\parallel*}$.

The fact that the stabilization of the manifold is prioritized over the movement on the manifold is illustrated in Fig. 5. In the upper part of this figure, the components of u^{1*} are shown which is calculated according to (25) but using all quantities from OCP1, i.e.,

$$u^{1*}(t) = \kappa \left(\xi^*(t), \eta^{1*}(t), v^{\text{th}*}(t), v^{\parallel 1*}(t) \right). \quad (55)$$

In the lower part of Fig. 5, the optimal solutions $v^{\parallel 1*}$ from OCP1 and $v^{\parallel*}$ from OCP2 are depicted.

During the time interval $[0, 0.75]$ s the optimal solution of OCP1 is such that all input constraints are active which results in the fact that there is no remaining margin for OCP2 to achieve the desired tangential movement. This is clearly visible as the corresponding components of $v^{\parallel 1*}$, which is not based on any optimality criterion regarding the tangential movement, and $v^{\parallel*}$ are identical over the time interval $[0, 0.75]$ s. Moreover, as a result η_3^* is even getting larger. As soon as one or more input constraints become inactive, the solutions $v^{\parallel 1*}$ and $v^{\parallel*}$ differ in one or more components, which is also visible in Fig. 5. The tangential movement can then be influenced in a specific way and, in particular, η_3^* approaches zero. Note that due to Assumption 14, this has to happen sooner or later. The convergence to the manifold

implies that ξ^* reaches the region $\Omega_{\mathcal{M}}^\varepsilon$ around the manifold where, according to Assumption 14, inputs exist which simultaneously drive the system to the manifold and achieve a desired movement on the manifold, both under due consideration of the input constraints.

In the following, the properties of the proposed control concept are further highlighted. This is done by a comparison with a model predictive controller based on the single OCP

$$\min_{\bar{v}^{\text{th}}(\cdot), \bar{v}^{\parallel}(\cdot)} J^{\text{th}}(t_k, \bar{v}^{\text{th}}(\cdot)) + J^{\parallel}(t_k, \bar{v}^{\parallel}(\cdot)) \quad (56a)$$

$$\text{s.t.} \quad (19b)-(19f) \quad (56b)$$

which is solved at each sampling instant t_k . Apart from the cost functional (56a) it is identical to OCP1. In the OCP (56) the cost functionals dedicated to the transverse and tangential movement are added up and the sum is minimized. At first glance, this appears to be a reasonable strategy for stabilizing the manifold and achieving a desired tangential movement on it. The input applied to the system is calculated from the optimal solution of (56) in the form

$$u(t) = \kappa \left(\bar{\xi}^*(t), \bar{\eta}^*(t), \bar{v}^{\text{th}*}(t), \bar{v}^{\parallel*}(t) \right), \quad t \in [t_k, t_{k+1}). \quad (57)$$

All parameter values of the OCP (56) are the same as for the proposed controller with two OCPs.

For the model predictive controller based on (56) and the same initial condition $x_0 = [0.1 \ 0.45 \ 2 \ 0 \ 0 \ -2]^T$ as before, the resulting trajectory of the closed-loop system of the point-like mass can be seen in Fig. 6 from two different viewpoints. By comparing it with the solid line in Fig. 1, the prioritization resulting from the structure with two sequentially solved OCPs becomes immediately visible. When using the proposed controller, the particle stays much closer to the manifold (after compensating for the initial deviation) compared to the case when just a single OCP is solved at each sampling instant. For the latter a compromise situation occurs inducing that the particle is directly moved toward $x_3 = 0$. On the contrary, the proposed controller with two OCPs primarily aims at driving the point-like mass to the manifold which can be accomplished better with a slight excursion of x_3 in positive direction.

Besides the prioritization, the most important reason for choosing the structure with two OCPs is given by the invariance property. This reasoning can be further substantiated by another comparison with the model predictive controller based on the single OCP (56). To this end, it is executed for the initial condition $x_0 = [0.5 \ 0 \ 2 \ 0 \ 2a + d \sin(2c) \ 0]^T$ which also served previously for demonstrating the invariance property. Fig-

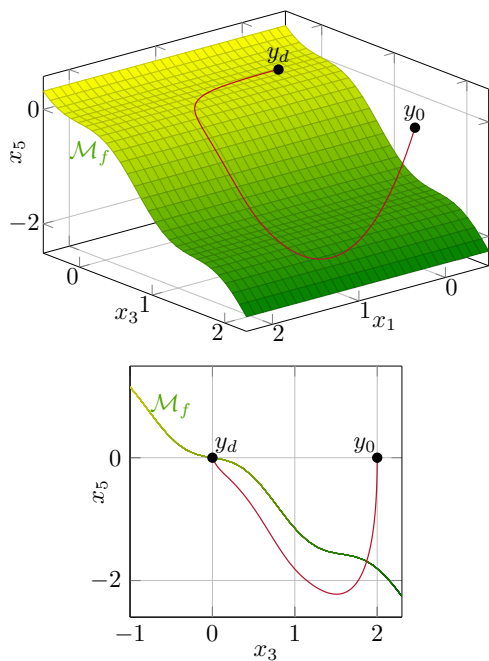


Fig. 6. Trajectory of the particle and \mathcal{M}_f for the controller based on a single OCP.

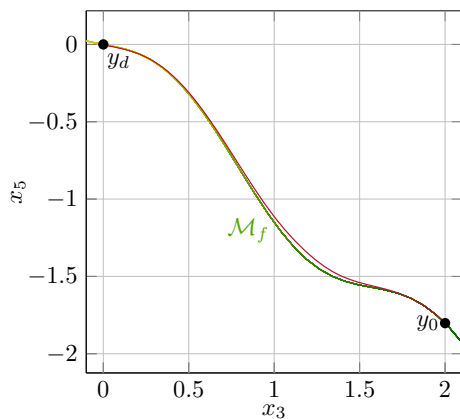


Fig. 7. Trajectory of the particle and \mathcal{M}_f for the controller based on a single OCP and the initial condition corresponding to a position of rest exactly on \mathcal{M}_f .

Figure 7 shows the corresponding trajectory of the particle in closed loop. The inputs to the system for the proposed control strategy and the controller based on just a single OCP are displayed in Figs. 8 and 9, respectively. For both controllers, the input constraints become active. However, the model predictive controller based on a single OCP violates the invariance property which can be seen in Fig. 7 as the point-like mass leaves the manifold \mathcal{M}_f . This is not the case for the proposed control concept (cf. the dash-dot line in Fig. 1) which clearly justifies the structure with two sequentially solved OCPs. Obvi-

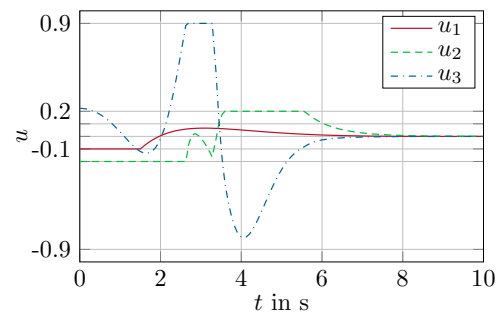


Fig. 8. System inputs u for the controller with two OCPs and the initial condition corresponding to a position of rest exactly on \mathcal{M}_f .

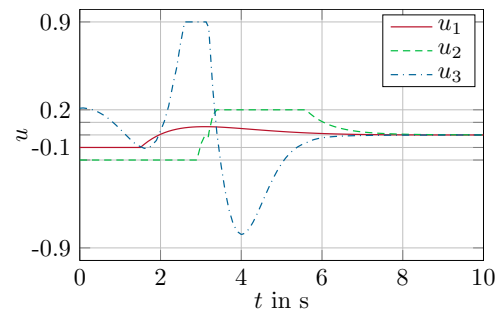


Fig. 9. System inputs u for the controller based on a single OCP and the initial condition corresponding to a position of rest exactly on \mathcal{M}_f .

ously, for the controller based on a single OCP a compromise situation occurs, i.e., the increase of the value of the cost functional (56a) due to leaving the manifold can be counterbalanced with a better performance in tangential direction. The main difference in the behavior is also well visible at the control input u_2 for both controllers in Figs. 8 and 9. The model predictive controller based on two OCPs increases u_2 slightly earlier than the one based on a single OCP. This reduces the velocity in negative x_3 direction and enables to hold the particle on the manifold. Despite this reduction of the velocity, the overall maneuver is accomplished at virtually the same time.

Remark 20 *The simple example of a point-like mass has been chosen to emphasize the application of the proposed concept and the corresponding determination of the controller parameters. Nevertheless, the presented control scheme can be directly applied to more elaborate systems without facing any further problems.*

7 Conclusion

The stabilization of manifolds under system constraints was investigated. To this end, the concept of transverse normal forms is used in combination with a novel model

predictive control scheme. In contrast to existing concepts in the literature, two optimal control problems are sequentially solved at each sampling instant. This enables to prioritize the movement to the manifold over the movement on the manifold. Furthermore, no compromise between the weighting of the transverse and tangential movement in the cost functional has to be taken. One possibility was pointed out for proving convergence of the proposed control concept. Its applicability was shown by an illustrative simulation example.

Current work is dedicated to the mathematical formulation of the prioritization property. In addition, the application of the proposed control scheme to more complex systems is planned.

A Auxiliary calculations for the proof of Theorem 16

For brevity, the argument (t) is omitted in the following. Furthermore, where necessary, the shortcut T_k is used for $t_k + T$. By integrating (29) from $t_k + T$ to $t_k + s + T$ one obtains

$$V^{\hat{\eta}} \left(\Phi_{t_k+s+T}^{\xi_s} \right) - V^{\hat{\eta}} \left(\Phi_{t_k+T}^{\xi_s} \right) + \int_{t_k+T}^{t_k+s+T} l^{\hat{\eta}} \left(\Phi_t^{\xi_s}, \hat{v}^{\hat{\eta}} \right) dt \leq 0 \quad (\text{A.1a})$$

$$V^{\parallel} \left(\Phi_{t_k+s+T}^{\eta_s} \right) - V^{\parallel} \left(\Phi_{t_k+T}^{\eta_s} \right) + \int_{t_k+T}^{t_k+s+T} l^{\parallel} \left(\Phi_t^{\eta_s}, \hat{v}^{\parallel} \right) dt \leq 0. \quad (\text{A.1b})$$

The right-hand side of (33) can be written as

$$\begin{aligned} & J^{\hat{\eta}} \left(t_k + s, \hat{v}^{\hat{\eta}}(\cdot) \right) + J^{\parallel} \left(t_k + s, \hat{v}^{\parallel}(\cdot) \right) = \\ & \underbrace{\int_{t_k+s}^{t_k+T} l^{\hat{\eta}} \left(\Phi_t^{\xi_s}, \hat{v}^{\hat{\eta}} \right) dt + \int_{t_k}^{t_k+s} l^{\hat{\eta}} \left(\bar{\xi}^*, \bar{v}^{\hat{\eta}*} \right) dt + V^{\hat{\eta}} \left(\bar{\xi}^*(T_k) \right)}_{J^{\hat{\eta}}(t_k, \bar{v}^{\hat{\eta}*}(\cdot))} \\ & + \underbrace{\int_{t_k+s}^{t_k+T} l^{\parallel} \left(\Phi_t^{\eta_s}, \hat{v}^{\parallel} \right) dt + \int_{t_k}^{t_k+s} l^{\parallel} \left(\bar{\eta}^*, \bar{v}^{\parallel*} \right) dt + V^{\parallel} \left(\bar{\eta}^*(T_k) \right)}_{J^{\parallel}(t_k, \bar{v}^{\parallel*}(\cdot))} \\ & + \underbrace{\int_{t_k+T}^{t_k+s+T} l^{\hat{\eta}} \left(\Phi_t^{\xi_s}, \hat{v}^{\hat{\eta}} \right) dt + V^{\hat{\eta}} \left(\Phi_{t_k+s+T}^{\xi_s} \right) - V^{\hat{\eta}} \left(\bar{\xi}^*(T_k) \right)}_{\leq 0 \text{ due to (A.1a)}} \\ & + \underbrace{\int_{t_k+T}^{t_k+s+T} l^{\parallel} \left(\Phi_t^{\eta_s}, \hat{v}^{\parallel} \right) dt + V^{\parallel} \left(\Phi_{t_k+s+T}^{\eta_s} \right) - V^{\parallel} \left(\bar{\eta}^*(T_k) \right)}_{\leq 0 \text{ due to (A.1b)}} \end{aligned}$$

$$- \int_{t_k}^{t_k+s} l^{\hat{\eta}} \left(\bar{\xi}^*, \bar{v}^{\hat{\eta}*} \right) dt - \int_{t_k}^{t_k+s} l^{\parallel} \left(\bar{\eta}^*, \bar{v}^{\parallel*} \right) dt \quad (\text{A.2})$$

resulting in (34).

References

- [1] Adeel Akhtar, Steven L. Waslander, and Christopher Nielsen. Path following for a quadrotor using dynamic extension and transverse feedback linearization. In *Proc. 51st IEEE Conference on Decision and Control*, pages 3551–3556, Maui, HI, USA, December 2012.
- [2] Francesca Albertini and Eduardo D. Sontag. Continuous control-Lyapunov functions for asymptotically controllable time-varying systems. *International Journal of Control*, 72(18):1630–1641, 1999.
- [3] Frank Allgöwer, Thomas A. Badgwell, Joe S. Qin, James B. Rawlings, and Stephen J. Wright. Nonlinear predictive control and moving horizon estimation – An introductory overview. In Paul M. Frank, editor, *Advances in Control: Highlights of ECC '99*, pages 391–449. Springer, 1999.
- [4] Martin Böck and Andreas Kugi. Manifold stabilization and path-following control for flat systems with application to a laboratory tower crane. In *Proc. 53rd IEEE Conference on Decision and Control*, pages 4529–4535, Los Angeles, CA, USA, December 2014.
- [5] Martin Böck and Andreas Kugi. Real-time nonlinear model predictive path-following control of a laboratory tower crane. *IEEE Transactions on Control Systems Technology*, 22(4):1461–1473, 2014.
- [6] Hong Chen. *Stability and Robustness Considerations in Nonlinear Model Predictive Control*. Number 674 in Fortschritt-Berichte VDI, Reihe 8: Meß-, Steuerungs- und Regelungstechnik. VDI Verlag, 1997.
- [7] Hong Chen and Frank Allgöwer. A quasi-infinite horizon nonlinear model predictive control scheme with guaranteed stability. *Automatica*, 34(10):1205–1217, 1998.
- [8] Dragan B. Dačić, Dragan Nešić, and Petar V. Kokotović. Path-following for nonlinear systems with unstable zero dynamics. *IEEE Transactions on Automatic Control*, 52(3):481–487, 2007.
- [9] Emmanuel Delaleau and Joachim Rudolph. Control of flat systems by quasi-static feedback of generalized states. *International Journal of Control*, 71(5):745–765, 1998.
- [10] Charles A. Desoer and Mathukumalli Vidyasagar. *Feedback Systems: Input-Output Properties*. Electrical Science. Academic Press, 1975.
- [11] Mohamed Ibrahim El-Hawwary. *Passivity methods for the stabilization of closed sets in nonlinear control systems*. PhD thesis, University of Toronto, Canada, 2011.
- [12] Mohamed Ibrahim El-Hawwary and Manfredi Maggiore. Reduction principles and the stabilization of closed sets for passive systems. *IEEE Transactions on Automatic Control*, 55(4):982–987, 2010.
- [13] Pedro Encarnação and António Pascoal. Combined trajectory tracking and path following: an application to the coordinated control of autonomous marine craft. In *Proc. 40th IEEE Conference on Decision and Control*, pages 964–969, Orlando, FL, USA, December 2001.

- [14] Timm Faulwasser and Rolf Findeisen. Constrained output path-following for nonlinear systems using predictive control. In *Proc. 8th IFAC Symposium on Nonlinear Control Systems*, pages 753–758, Bologna, Italy, September 2010.
- [15] Timm Faulwasser, Benjamin Kern, and Rolf Findeisen. Model predictive path-following for constrained nonlinear systems. In *Proc. 48th IEEE Conference on Decision and Control and 28th Chinese Control Conference*, pages 8642–8647, Shanghai, P.R. China, December 2009.
- [16] Rolf Findeisen. *Nonlinear Model Predictive Control: A Sampled-Data Feedback Perspective*. PhD thesis, University of Stuttgart, Germany, 2004.
- [17] Rolf Findeisen, Lars Imsland, Frank Allgöwer, and Bjarne Foss. Towards a sampled-data theory for nonlinear model predictive control. In Wei Kang, Mingqing Xiao, and Carlos Borges, editors, *New Trends in Nonlinear Dynamics and Control, and their Applications*, volume 295 of *Lecture Notes in Control and Information Sciences*, pages 295–311. Springer, 2003.
- [18] Fernando A. C. C. Fontes. A general framework to design stabilizing nonlinear model predictive controllers. *Systems & Control Letters*, 42(2):127–143, 2001.
- [19] Lars Imsland and Bjarne A. Foss. State feedback set stabilization for a class of nonlinear systems. In Luca Benvenuti, Alberto De Santis, and Lorenzo Farina, editors, *Positive Systems: Proceedings of the First Multidisciplinary International Symposium on Positive Systems: Theory and Applications (POSTA 2003), Rome, Italy, August 28–30, 2003*, volume 294 of *Lecture Notes in Control and Information Sciences*, pages 337–344. Springer, 2003.
- [20] Alberto Isidori. *Nonlinear Control Systems*. Communications and Control Engineering. Springer, 3 edition, 1995.
- [21] Ali Jadbabaie and John Hauser. On the stability of receding horizon control with a general terminal cost. *IEEE Transactions on Automatic Control*, 50(5):674–678, 2005.
- [22] Christopher M. Kellett and Andrew R. Teel. Uniform asymptotic controllability to a set implies locally Lipschitz control-Lyapunov function. In *Proc. 39th IEEE Conference on Decision and Control*, volume 4, pages 3994–3999, Sydney, Australia, December 2000.
- [23] Hassan K. Khalil. *Nonlinear Systems*. Prentice Hall, 2 edition, 1996.
- [24] Denise Lam, Chris Manzie, and Malcolm C. Good. Model predictive contouring control. In *Proc. 49th IEEE Conference on Decision and Control*, pages 6137–6142, Atlanta, GA, USA, December 2010.
- [25] David Q. Mayne, James B. Rawlings, Christopher V. Rao, and Pierre O. M. Scokaert. Constrained model predictive control: Stability and optimality. *Automatica*, 36(6):789–814, 2000.
- [26] Sergey G. Nersesov, Parham Ghorbanian, and Amir G. Aghdam. Stabilization of sets with application to multi-vehicle coordinated motion. *Automatica*, 46(9):1419–1427, 2010.
- [27] Chris Nielsen and Manfredi Maggiore. Maneuver regulation via transverse feedback linearization: Theory and examples. In *Proc. 6th IFAC Symposium on Nonlinear Control Systems*, volume 1, pages 57–64, Stuttgart, Germany, September 2004.
- [28] Christopher Nielsen. *Set Stabilization Using Transverse Feedback Linearization*. PhD thesis, University of Toronto, Canada, 2009.
- [29] Christopher Nielsen, Cameron Fulford, and Manfredi Maggiore. Path following using transverse feedback linearization: Application to a maglev positioning system. *Automatica*, 46(3):585–590, 2010.
- [30] Christopher Nielsen and Manfredi Maggiore. On local transverse feedback linearization. *SIAM Journal on Control and Optimization*, 47(5):2227–2250, 2008.
- [31] James B. Rawlings and David Q. Mayne. *Model Predictive Control: Theory and Design*. Nob Hill Publishing, 2009.
- [32] Marcus Reble and Frank Allgöwer. Unconstrained model predictive control and suboptimality estimates for nonlinear continuous-time systems. *Automatica*, 48(8):1812–1817, 2012.
- [33] Anton S. Shiriaev. The notion of V -detectability and stabilization of invariant sets of nonlinear systems. *Systems & Control Letters*, 39(5):327–338, 2000.
- [34] Anton S. Shiriaev and Alexander L. Fradkov. Stabilization of invariant sets for nonlinear non-affine systems. *Automatica*, 36(11):1709–1715, 2000.
- [35] Roger Skjetne, Thor I. Fossen, and Petar V. Kokotović. Robust output maneuvering for a class of nonlinear systems. *Automatica*, 40(3):373–383, 2004.
- [36] Roger Skjetne, Andrew R. Teel, and Petar V. Kokotović. Stabilization of sets parametrized by a single variable: Application to ship maneuvering. In *Proc. 15th International Symposium on the Mathematical Theory of Networks and Systems*, South Bend, IN, USA, August 2002.
- [37] Kevin Casey Walker. *Surface Geometry and the Haptic Rendering of Rigid Point Contacts*. PhD thesis, University of Waterloo, Canada, 2013.
- [38] Shuyou Yu, Xiang Li, Hong Chen, and Frank Allgöwer. Nonlinear model predictive control for path following problems. In *Proc. 4th IFAC Nonlinear Model Predictive Control Conference*, pages 145–150, Noordwijkerhout, The Netherlands, August 2012.